

Impact of rural depopulation and climate change on vegetation, runoff and sediment load in the Gan River basin, China

Lidong Huang, Aizhong Ye, Chongjun Tang, Qingyun Duan and Yahai Zhang

ABSTRACT

Climate change and rural depopulation are changing the ecological and hydrological cycles in China. Data on the normalized difference vegetation index (NDVI), temperature, precipitation, streamflow, sediment and rural population are available for the Gan River basin from 1981 to 2017.

We investigated the spatio-temporal variations in climate, human activity and vegetation mainly using the Mann–Kendall test and examined their relationship using the Granger causality test. The results showed that (1) the temperature markedly increased in all seasons; (2) the precipitation increased in summer and winter but decreased in spring and autumn; (3) overall, the NDVI increased markedly during 2005–2017, but showed seasonal differences, with decreases in summer and winter and increases in spring and autumn; (4) the annual sediment transport showed a significant decreasing trend and (5) a large number of the population shifted from rural to urban areas, resulting in a decrease in the rural population between 1998 and 2018. Rural depopulation has brought about farmland abandonment, conversion of farmland to forests, which was the factor driving the recovery of the vegetation and the decrease in sediment. The results of this study can provide support for climate change adaptation and sustainable development.

Key words | climate change, eco-hydrology effects, Granger causality test, rural depopulation

HIGHLIGHTS

- The temperature markedly increased in all seasons.
- The precipitation increased in summer and winter but decreased in spring and autumn.
- The NDVI increased markedly during 2005 to 2017.
- The annual sediment transport showed a significant decreasing trend.
- A large number of the population shifted from rural to urban areas.

INTRODUCTION

According to the Intergovernmental Panel on Climate Change (IPCC) Fifth Assessment Report (AR5), global climate change is unquestionable. The urbanization process

has also been developing rapidly over the past 30 years in China. Urbanization is a dynamic process generated by the population exchange from rural to urban areas through internal migration (Ledent & Jacques 1982). The United Nations predicts that population growth of urban areas will represent the bulk of the world's projected population growth, rising to 6.3 billion by 2050 (While & Whitehead

This is an Open Access article distributed under the terms of the Creative Commons Attribution Licence (CC BY 4.0), which permits copying, adaptation and redistribution, provided the original work is properly cited (<http://creativecommons.org/licenses/by/4.0/>).

doi: 10.2166/nh.2020.120

Lidong Huang

Aizhong Ye (corresponding author)

Qingyun Duan

Yahai Zhang

State Key Laboratory of Earth Surface and Ecological Resources, Faculty of Geographical Science,

Beijing Normal University,

Beijing 100875,

China

E-mail: azyebnu.edu.cn

Chongjun Tang

Key Laboratory of Soil Erosion and Prevention of

Jiangxi Province,

Jiangxi Institute of Soil and Water Conservation,

Nanchang 330029,

China

2013). Additionally, some developed countries in Asia will experience a very high rate of urbanization between 2005 and 2030 (Jacobson 2011). China's urbanization rate reached 57.35% in 2016, indicating that 792.98 million people live in cities and towns according to the National Bureau of Statistics of China. Both climate change and urbanization affect the terrestrial surface system in which humans live, while the ecological and hydrological cycles play an important role in the terrestrial surface system (Pumo *et al.* 2017). In recent years, the impacts of climate change and urbanization on eco-hydrological processes have been the focus of research (Wei *et al.* 2013; Cristea *et al.* 2014; Hagemann *et al.* 2014; Sellami *et al.* 2015; Pumo *et al.* 2017; Qi *et al.* 2019; Zhang *et al.* 2019).

The influence of climate change on vegetation is different in different climatic zones. The increase in summer temperature leads to drought, which is unfavorable to vegetation growth in arid areas (Tang *et al.* 2016). And the precipitation rate is the main limiting factor affecting vegetation growth in arid and semi-arid regions (Cai *et al.* 2014). Furthermore, vegetation cover change will have complex impacts on the local hydrological process. The relative intensity of interception, infiltration and evapotranspiration resulting from vegetation change in different places is different, and the effect of vegetation cover change on runoff production is also different (Price 2011). Urbanization will lead to rural depopulation and land-use change (Salvadore *et al.* 2015; Leroux *et al.* 2017; Liu *et al.* 2019). The urban land cover change could lower water permeability and increase runoff and evapotranspiration (Leopold 1968; Doyle *et al.* 2000; Jacobson 2011; Salvadore *et al.* 2015). A large number of rural people moving into cities results in abandoned arable land in China (Shao *et al.* 2016). The land abandonment changes the carbon content (Novara *et al.* 2017) and hydraulic conductivity of the soil, further affects infiltration and runoff (Cerdà 1997; Di Prima *et al.* 2018), and increases soil organic matter, restores vegetation (Cerdà *et al.* 2018) and reduces soil loss (Cerdà *et al.* 2019). The Sustainable Development Goals related to the sustainable development goals of food, water and climate proposed by the United Nations require us to attach importance to the study of land-use change (Keesstra *et al.* 2018) and help strengthen sustainable land use and management (Keesstra *et al.* 2016).

In order to quantify the specific causal relationship between eco-hydrological elements and human activities and climate change, the Granger causality test (GCT) can be used as a reference method. The GCT (Granger 1969), which was first proposed in 1969 by Clive W. Granger, the Nobel laureate in economics, defines causality as 'the ability of a priori value of one time series to predict another time series' when predicting the future of a set of data. If predicting future information using the past information of another set of data is better than using only that data itself, then there is a Granger causality between the two sets of data (Papagiannopoulou *et al.* 2017).

Granger causality should not be interpreted as 'real causality'. To simplify, one assumes that if the past of a time series A is helpful in predicting the future of a time series B, A Granger causes B. This kind of analysis has been commonly applied in attribution analysis to investigate the influence of one variable on another. Papagiannopoulou *et al.* (2017) investigated the Granger-causal relation between climatic variables and NDVI, while Attanasio *et al.* (2012) applied the GCT to times series of natural/anthropogenic forcings and global temperature anomalies. Furthermore, Attanasio *et al.* (2013) investigated a Granger-causal relationship between greenhouse gases and temperature. In addition, Kaufmann *et al.* (2007) analyzed the causal influence of urbanization and enlargement of towns on precipitation in a Chinese case study.

In China, how do ecological and hydrological conditions change in the context of climate change and rural depopulation? What impact do climate change and rural depopulation have on the eco-hydrological process? In this study, data for precipitation, temperature, population, normalized difference vegetation index (NDVI), runoff and sediment load were available for the Gan River basin from 1981 to 2017. The trend and relationship of eco-hydrological factors will be analyzed to determine the impact of rural depopulation and climate change on the ecological and hydrological processes by using the Mann-Kendall (M-K) test and the GCT.

The organization of the paper is as follows: The next section describes the study area and data; the following two sections introduce the methodologies and present the results and discussion; and the final section provides the conclusions.

STUDY AREA AND DATA

Study area

The Gan River (24°29' to 29°11'N, 113°30' to 116°40'E) is located in Jiangxi Province in southeast China (Figure 1).

The Gan River is a tributary of the Yangtze River, with a drainage area of 82,809 km², occupying more than 50% of Jiangxi Province (Zhang *et al.* 2016a, 2016b). The Gan River basin is in a humid subtropical monsoon climate zone with abundant precipitation and frequent heavy rain. The mean annual precipitation is about 1,505 mm (1981–2016), and the mean

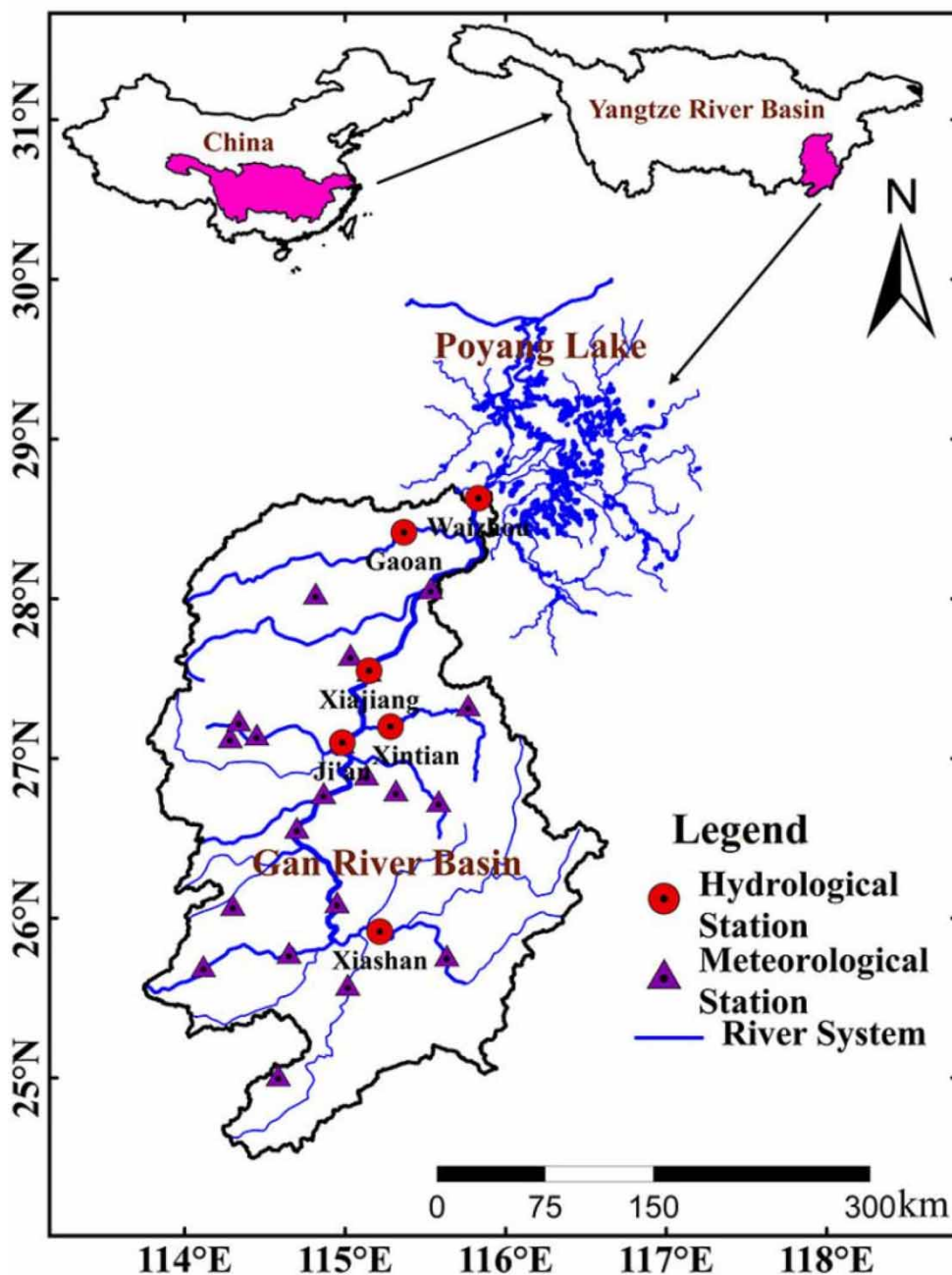


Figure 1 | Location of the Gan River basin and hydro-meteorological stations.

annual temperature is 17.9 °C (1981–2016), with distinct seasonal variations (Zhang *et al.* 2017). The total mean annual streamflow of the Gan River is approximately 68.7 billion m³, accounting for 50% of the total streamflow in the Poyang Lake basin (Chen *et al.* 2014). The annual average runoff coefficient value is 0.54 (Liu 2016).

In the 1980s, China's urbanization began to accelerate. The urbanization rate in Jiangxi Province increased from 16.8% in 1978 to 51.6% in 2015 (Ding 2017). While the surrounding areas of the Gan River basin (such as the Yangtze River Delta and the Pearl River Delta) are urbanizing even faster. This results in a large number of people in the Gan River basin migrating to the more developed surrounding areas. In addition, the development is uneven in the Gan River basin. The population is gradually concentrated in the more developed urban areas of the basin. All of these have led to a sharp decline in the agricultural population in the basin. Before the 1980s, the ecological environment of the Gan River basin was seriously damaged, and soil erosion was serious due to developing agriculture and obtaining firewood. Since 1980s, the ecological and hydrological conditions have been gradually improved. The forest coverage rate increased from 34.73% in the late 1983 to 63.10% in 2010 in Jiangxi Province according to the Jiangxi Statistical Yearbook in 2011. Therefore, this paper chooses the Gan River basin as the research area.

Data

Global Inventory Modelling and Mapping Studies (GIMMS) NDVI and MODIS NDVI (MOD13A) data were used in this study.

The GIMMS NDVI dataset is available from 1981 to 2006 at a spatial resolution of 8 km with 15-day intervals. The dataset is provided by Environmental and Ecological Science Data Center for West China, National Natural Science Foundation of China (<http://westdc.westgis.ac.cn/data/1cad1a63-ca8d-431a-b2b2-45d9916d860d>). The 1-km MOD13A3 product is released every month and was downloaded from <https://ladsweb.modaps.eosdis.nasa.gov/> for the period of 2000–2017. Observations from GIMMS were temporally synthesized to monthly maximum value to match the monthly temporal resolution of MODIS.

For analyzing the long-term dynamics of high-quality data, linear regression was applied to monthly MODIS NDVI and

GIMMS NDVI data that were averaged over the entire study area. When using the temporal overlap (2000.2–2006.12) of monthly GIMMS and MODIS, the data fitting was reliable ($R^2 > 0.7$), as shown in Figure 2. These are spatially averaged values of NDVI for the entire basin for each month, and 83 points are on the scatter plot (Figure 2). Compared with other sensors, the MODIS sensor offers improved features to monitor terrestrial vegetation (Fensholt & Proud 2012; Fan & Liu 2016). Here, the monthly GIMMS NDVI data (1981.1–2000.2) of each pixel were modified according to the linear regression equation in Figure 2. Then, the seasonal mean NDVIs were averaged by season, with spring including months from March to May, summer from June to August, autumn from September to November, and winter from December to February of the following year.

The gridded daily precipitation and temperature observations for 1981–2016 at a 0.5° resolution were obtained from the National Meteorological Information Center, CMA (<http://data.cma.cn/>). Considering that NDVI and meteorological data had different spatial resolutions, in order to unify the spatial scales of analysis, the Gan River basin was divided into 329 sub-basins based on the digital elevation model (DEM) data (<https://eros.usgs.gov/>). All data were analyzed at the sub-basin scale, and the sub-basin was taken as the smallest research unit. The daily

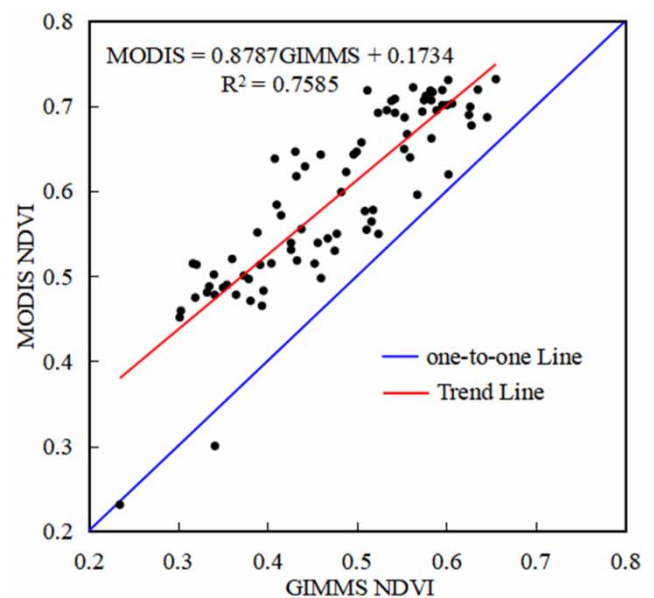


Figure 2 | The correlation between averaged monthly MODIS NDVI and GIMMS NDVI in the entire Gan River basin from 2000 to 2006.

streamflow datasets (1981–2013) were obtained from the Hydrological Yearbook. The yearly sediment data (1981–2013) were gathered from five articles on sediment transport research in the Gan River basin (Deng 2010; Zheng et al. 2012; Peng 2015; Liu 2016; Mo et al. 2017). This paper took the average of these five sets of data as reference data. The yearly rural population data (1985–2016) were obtained from the Jiangxi Statistical Yearbook. The investment data from the Soil and Water Conservation (e.g., total investment during the period of 1983–2005, yearly investment from 2008 to 2015) were obtained from the Bulletin of Soil and Water Conservation in Jiangxi Province. The urban and rural population dataset in 2000 was based on a quantitative model (Mao et al. 2012). The gross domestic product (GDP) data for 2000 was from the Data Center for Resources and Environmental Sciences of the Chinese Academy. The specific information can be seen in Table 1.

Figure 3 shows the physical and geographical conditions (e.g., altitude, spatial distribution of precipitation and temperature) and socioeconomic conditions of the Gan River basin in 2000. In general, the vegetation growth at the higher elevations of the Gan River basin is better, while the rural population is widely distributed in areas with relatively low altitudes near the outlet of the Gan River basin.

Table 1 | Information of basic data for the Gan River basin

Data type	Spatial resolution	Temporal resolution	Time range	Source
DEM	90 m	–	–	USGS (https://eros.usgs.gov/)
Precipitation	0.5° (≈55 km)	Daily	1981–2015	CMA (http://data.cma.cn/)
Temperature	–	Daily	1981–2016	
GIMMS NDVI	8 km	15 days	1981.11–2006.12	Environmental and Ecological Science Data Center for West China (http://westdc.westgis.ac.cn)
MODIS NDVI (MOD13A3)	1 km	Monthly	2000.2–2017.11	NASA LAADS DAAC (https://ladsweb.modaps.eosdis.nasa.gov/)
Discharge	–	Daily	1981–2013	Hydrological Yearbook
Sediment	–	Yearly	1981–2013	Deng (2010); Liu (2016); Mo et al. (2017); Peng (2015); Zheng et al. (2012)
Rural population	–	Yearly	1985–2016	Jiangxi Statistical Yearbook
Investment in soil and water conservation	–	–	The total investment from 1983 to 2005, yearly from 2008 to 2015	Bulletin of Soil and Water Conservation in Jiangxi Province
Urban and rural GDP and population	1 km	–	2000	Mao et al. (2012); Data Center for Resources and Environmental Sciences of the Chinese Academy

‘–’ means no data.

METHODOLOGIES

M–K test

In this paper, the M–K test was used to detect the trends in seasonal temperature, precipitation and NDVI. The M–K test is a nonparametric testing method (Mann 1945; Kendall 1955). Samples are not required to follow a certain distribution, nor are they interfered with by a few outliers. It is recommended and widely used by the World Meteorological Organization. Hence, it is suitable for non-normal distribution data in hydro-meteorological time series.

The statistic S is calculated using the following equations:

$$S = \sum_{k=1}^{n-1} \sum_{j=k+1}^n \text{sgn}(x_j - x_k) \quad (1)$$

$$\text{sgn}(x_j - x_k) = \begin{cases} 1 & (x_j - x_k) > 0 \\ 0 & (x_j - x_k) = 0 \\ -1 & (x_j - x_k) < 0 \end{cases} \quad (2)$$

$$E(S) = 0 \quad \text{var}(S) \approx \frac{n(n-1)(2n+5)}{18} \quad (3)$$

where $\{x_1, x_2, \dots, x_n\}$ is the time-series data, and n is the number of data points. $E(S)$ and $\text{var}(S)$ are the mean and variance of the statistic S , respectively. When $n > 10$, the

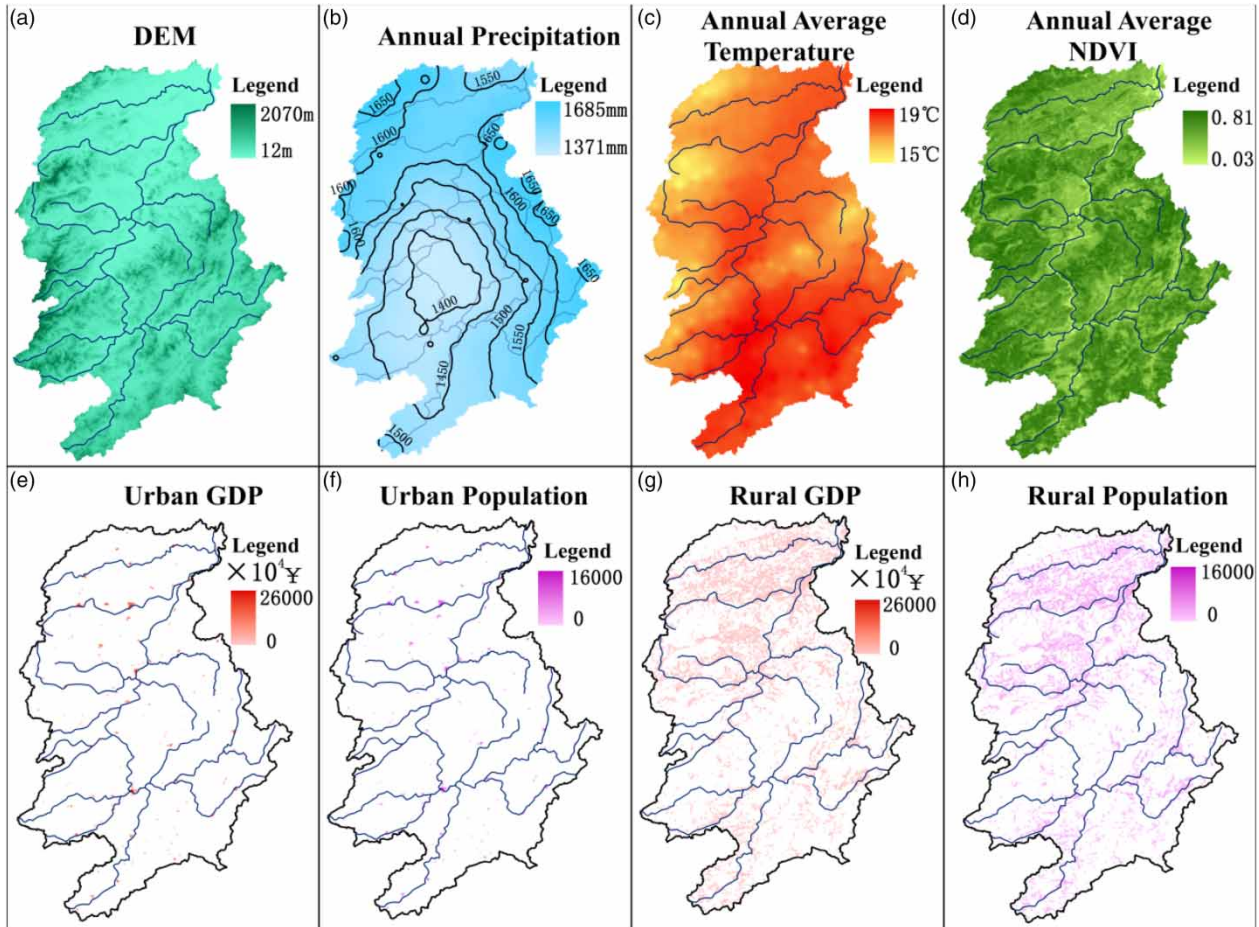


Figure 3 | The spatial distribution of natural and social conditions in the Gan River basin in 2000.

standard normal test statistic Z is computed using the following equation:

$$Z = \begin{cases} \frac{S-1}{\sqrt{\text{var}(S)}} & S > 0 \\ 0 & S = 0 \\ \frac{S+1}{\sqrt{\text{var}(S)}} & S < 0 \end{cases} \quad (4)$$

The statistic Z -value of the calculated time series is used to test the significance of trend statistics. A positive Z -value indicates an upward trend, while a negative Z -value shows a downward trend. When the absolute value of Z is greater than or equal to 1.28, 1.64 and 2.32, the significance tests of 90, 95, and 99% reliability are indicated, respectively.

Granger causality test (GCT)

In this paper, the GCT was mainly used to examine the causal relationships among the climatic factors, vegetation, water and sediment variables and socioeconomic factors.

The steps of the GCT are as follows:

Step 1: Test the stationarity of the time series X and Y . X and Y are cause and effect factors, respectively. The augmented Dick-Fuller test (ADF test) is generally used to test the stationarity of the time series X and Y by a unit root test (Dickey & Fuller 1979). If the time-series data are not stable, difference the time series to obtain a stationary series.

Step 2: Select a suitable lag term m , set up the auto-regressive model and calculate the residual sum of squares (RSS_R):

$$y_t = a_0 + \sum_{i=1}^m a_i y_{t-i} + \varepsilon_t \quad (5)$$

where the term y_t is the dependent variable at time t , a_0 is a constant term, a_i is the regression coefficient, and ε_t is the error term.

Step 3: Select the appropriate lag value q for time series X to establish the regression and calculate the residual sum of squares (RSS_{UR}):

$$y_t = a_0 + \sum_{i=1}^m a_i y_{t-i} + \sum_{i=1}^q b_i x_{t-i} + \varepsilon_t \quad (6)$$

Step 4: Assume that $H_0: b_1 = \dots = b_q = 0$. That is, lag items of all time series do not belong to the regression.

Step 5: Perform the F -test:

$$F = \frac{(RSS_R + RSS_{UR})/q}{RSS_{UR}/(n - m - q - 1)} \quad (7)$$

where n is the sample size.

Step 6: If the F -value under the significant level α is greater than the critical value F_α (obtained by looking up the F -test threshold table), the original hypothesis (H_0) is rejected; thus, the lag term of time series X belongs to this regression, which indicates that time series X is the Granger cause of time series Y . If the p -values obtained from the F -test are lower than a certain significance level (0.1 in this paper), the null hypothesis that Y fails to 'Granger cause' X can be rejected.

RESULTS AND DISCUSSION

Trend analysis of annual temperature, precipitation and NDVI

The Gan River basin was divided into 329 sub-basins based on the DEM data. All observed temperature, precipitation and NDVI data were interpolated to each sub-basin by the IDW method (inverse distance weighting method) (Shepard 1968). Figure 4 illustrates the trend of the seasonal average temperature in the Gan River basin during 1981–2016. All seasonal average temperatures, except the summer average temperature ($0 < Z < 1.28$), showed significant increasing trends ($Z > 1.28$) in almost the entire Gan River basin.

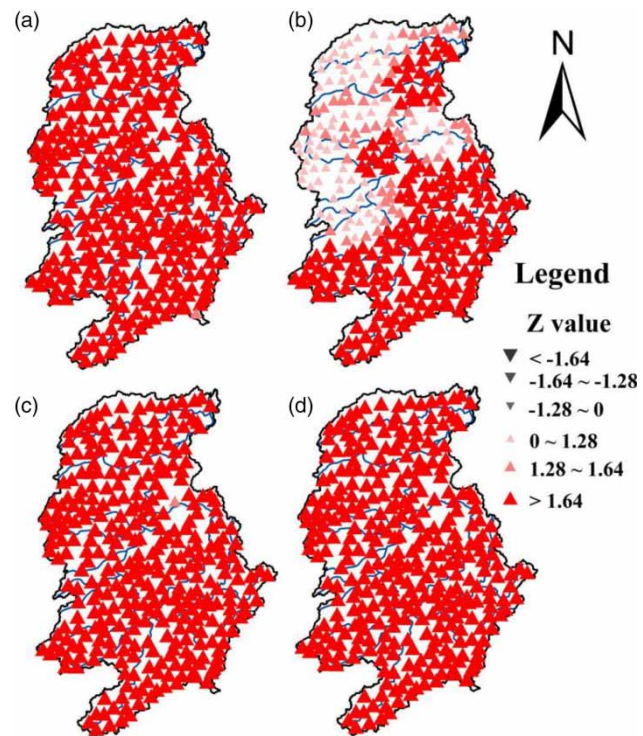


Figure 4 | M-K test trends of seasonal average temperature in the Gan River basin during the period 1981–2016. (a) Spring (March to May), (b) summer (June to August), (c) autumn (September to November) and (d) winter (December to February of the following year).

Figure 5 shows the spatial distribution of the seasonal precipitation trends. The precipitation of the Gan River basin in spring showed a decreasing trend except for the precipitation of the southern sub-basins, which increased non-significantly. In summer, the majority of the sub-basins in the north showed a non-significant increasing trend, while the southern sub-basins showed non-significant decreasing trends. In autumn, the precipitation of the northeastern corner of the Gan River basin, which is near the watershed outlet, showed a non-significant increasing trend, while the precipitation in all other sub-basins showed a decreasing trend. In winter, almost all of the sub-basins showed non-significant increasing trends.

The spatial distributions of trends of the NDVI in the Gan River basin are shown in Figure 6. The NDVI of the Gan River basin in spring showed an increasing trend in most sub-basins, especially in the central sub-basins. In summer, the NDVI tended to decrease along the Gan River riverway, and the decreasing trend was significant in

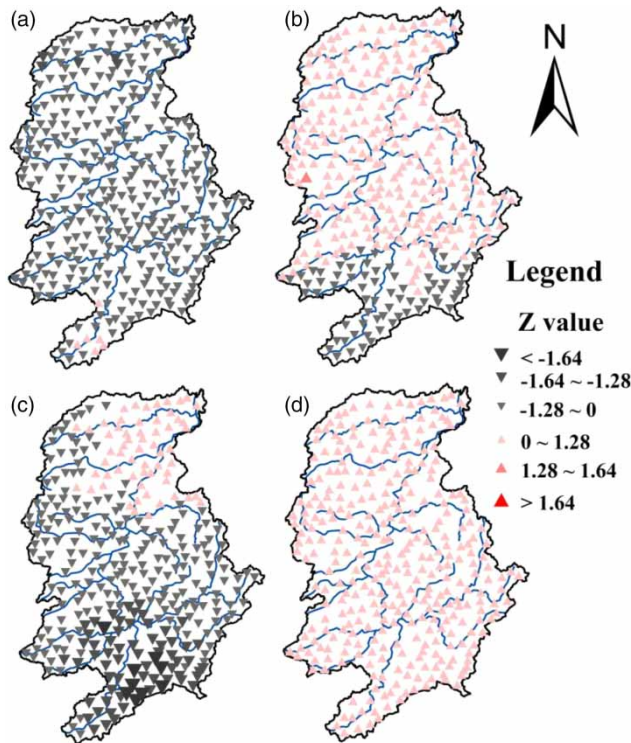


Figure 5 | Spatio-temporal changes in the seasonal precipitation in the Gan River basin during the period 1981–2015: (a) spring, (b) summer, (c) autumn, and (d) winter.

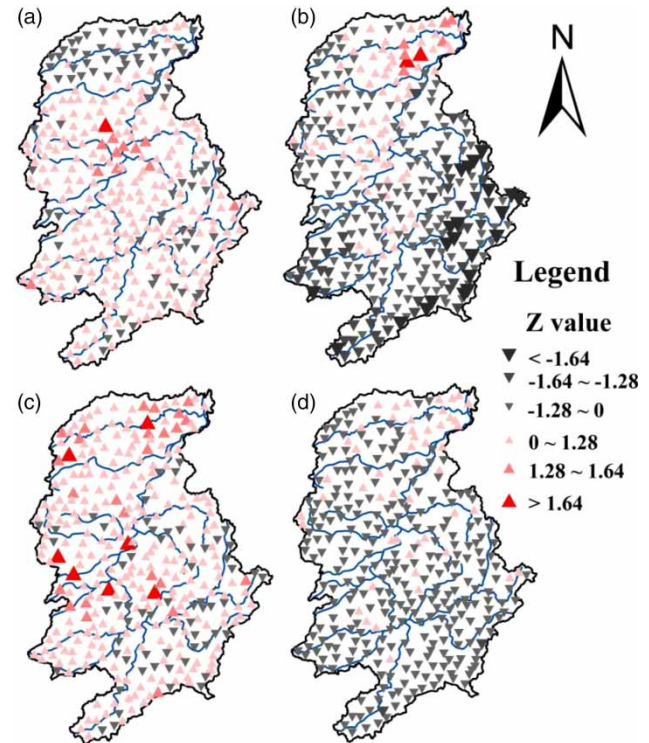


Figure 6 | M-K test trends of seasonal average NDVI in the Gan River basin during the period 1981–2017: (a) spring, (b) summer, (c) autumn, and (d) winter.

the southeastern and the southwestern sub-basins. The NDVI of almost all of the sub-basins showed an upward trend in autumn. The NDVI of most sub-basins showed a decreasing trend in winter. Comparing Figure 5 with Figure 6, it could be seen that corresponding seasonal precipitation and NDVI showed opposite trends. The possible reason was that the NDVI responded to precipitation with a time lag. Previous studies have shown a time-lag effect of vegetation responses to climatic factors (Anderson et al. 2010; Bai et al. 2012; Wu et al. 2015; Kong et al. 2018).

Rural depopulation in the Gan River basin, China

Urbanization refers to the population shift from rural to urban areas and the gradual increase in the proportion of people living in urban areas. The urbanization rate increased from 16.8% in 1978 to 51.6% in 2015 in the Gan River basin. The economic development level of cities within the Gan River basin was all lower than the average level of Jiangxi Province (Ding 2017). A large number of

rural laborers have gradually moved to places with higher levels of urbanization in the Gan River basin since the end of last century. Migrant workers working outside the province were mainly concentrated in the more developed Yangtze River Delta and Pearl River Delta regions. At the end of 2012, approximately 7.56 million workers of the total 19 million rural laborers in Jiangxi Province were employed outside the province (Qian 2014).

Thus, besides being under the influence of climate change, the Gan River basin is also affected by the process of rural depopulation. The following analyzes the specific features of the ecological and hydrological changes in the entire Gan River basin under these background conditions.

The runoff and sediment load change

Runoff and sediment characteristics play an important role in maintaining the regional environment and stabilizing the ecosystem (Wesselink et al. 2009). The Waizhou Hydrological Station is at the outlet of the Gan River basin. We applied the M-K test for the analysis of time-series trends

of water discharge and sediment load. A simple linear fitting of the dynamic process of runoff and sediment was performed. The results showed that the annual runoff had an unnoticeable change ($Z = 0.11$) in the Gan River basin, the annual sediment load showed a significant downward trend ($Z = -5.50$) since 1993 and decreased at a rate of 32.055×10^6 t/year (Figure 7).

Figure 7 indicates that the patterns of the dynamic changes in the sediment load and runoff were consistent, but the downward trends of the sediment load did not match the runoff after 1993. Therefore, the declining trend of the sediment load may be ascribed to human activities, such as the construction of reservoirs and dams and the reduction of sediment yield in the upper basin of the Gan River.

The impact of rural depopulation and climate change on the vegetation, runoff and sediment load

Soil erosion was very serious in the Gan River basin before the 1980s because of the destruction of vegetation caused by human activities. Since 1983, the country has adopted a series of ecological construction measures in the Gan River basin. Therefore, here, we have also considered the impact of the ecological conservation on the eco-hydrology of the Gan River basin.

Figure 8 presents the interannual variations of vegetation, runoff and sediment variables at the entire basin

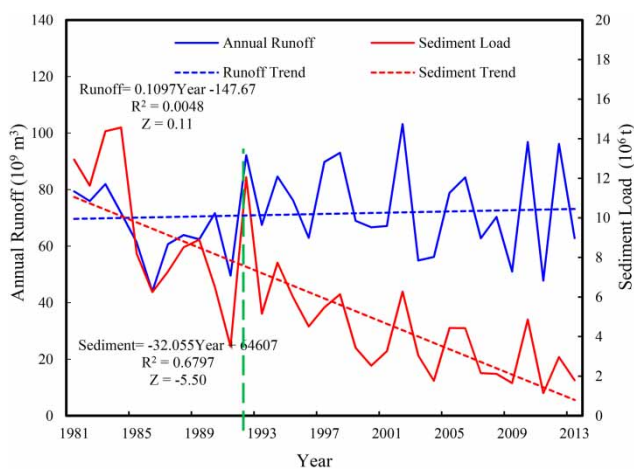


Figure 7 | Annual runoff and sediment load process at the Waizhou Hydrological Station from 1981 to 2013.

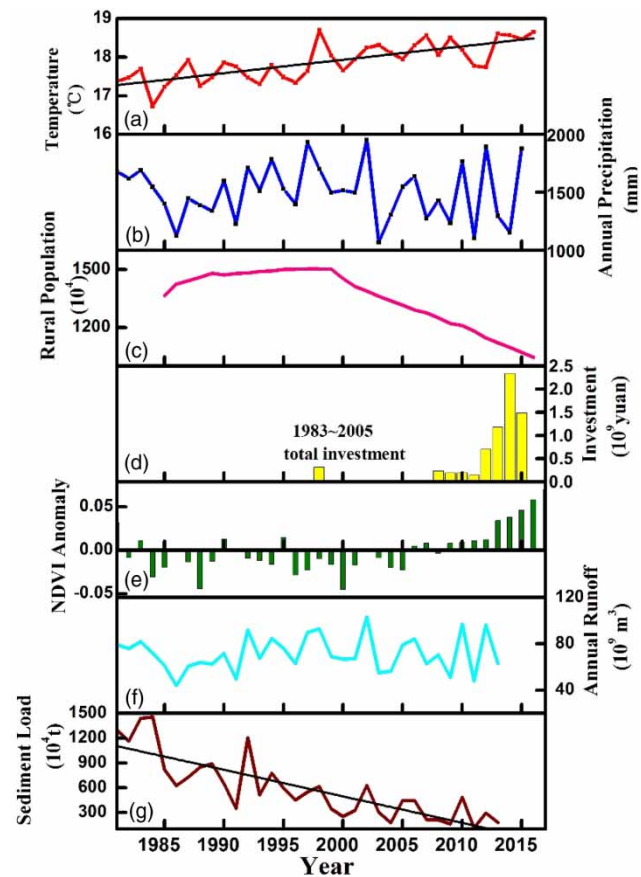


Figure 8 | Changes in (a) temperature, (b) annual precipitation, (c) rural population and (d) investment (since only the total investment data from 1983 to 2005 were obtained, the total investment in these years was plotted in the middle of the 1983-2005 period), (e) NDVI anomaly, (f) annual runoff, and (g) sediment load in the Gan River basin from 1981 to 2015.

scale since 1981 during the process of climate change, continuous rural depopulation, and implementation of the Soil and Water Conservation Project and other ecological construction programs.

Figure 8(c) shows that the rural population began to decline around the year 2000, which basically coincided with the emergence of an upsurge of migrant workers at the end of the 20th century. More than 4 million migrant workers in Jiangxi Province, an administrative unit within the Gan River basin, enter the metropolis every year. In 2003, the number of labor exports reached 4.6 million. By the end of 2012, there were 7.56 million migrant workers. The 70% were employed outside the province (Qian 2014). This directly led to a reduction in the rural population engaged in agricultural production, resulting in a shortage of farming labor and

abandonment of arable land. In 2000, the abandoned farmland area in Jiangxi Province was 433 km², which occupied approximately 2% of the existing arable land in the province. During the period of 2009–2014, more farmland was abandoned in Jiangxi Province, and the abandoned farmland area increased by 1,054 km² in 6 years (Liu 2016).

Figure 8(e) depicts that the annual mean NDVI anomalies before 2005 were negative but positive after 2005, that is, the annual mean NDVI in the Gan River basin began to exceed the multi-year average value in 2005, and the change trend of NDVI was relatively consistent with the rural population change during 2005–2017 (Figure 8(c)). Figure 8(a) shows that the temperature has been rising over the past 30 years, while the annual precipitation has not changed considerably (Figure 8(b)). The annual sediment load shows a sharp downward trend (Figure 8(g)). Precipitation and runoff are important factors influencing sediment load, and precipitation is the main factor affecting runoff in the Gan River basin (Liu 2016), but Figure 8(f) and 8(b) shows that precipitation and runoff changes are all small. The changes of NDVI and sediment load should be related to human activities, such as the rural depopulation and ecological protection project and the water conservancy project. In the Gan River basin, rural depopulation can reduce the frequency of human activities in rural areas, and also, this can reduce the activity of cutting down trees for firewood. There was 30.78 million tons of firewood used in 1985 in rural areas of Jiangxi Province (Qian 2014). Therefore, the large population moving out of the rural areas can reduce the damage to forest trees to a certain extent. The change of the NDVI also had a certain corresponding relationship with the investment intensity of ecological construction projects (Figure 8(d)). The implementation of these ecological projects is one of the main reasons for vegetation restoration. Rural population migration could cause abandonment of farmland. Some studies have shown that abandoned land can increase the content of organic matter and the infiltration ability of the soil, which help restore vegetation, weaken soil and water loss from the land surface, and restore the ecosystem (Romero *et al.* 2011; Romero-Díaz *et al.* 2016). The reduction of sediment load is also likely to be related to water conservancy project, and 4,355 reservoirs have been built in the Gan River (Liu 2016).

To further quantitatively analyze the relationship between rural depopulation/climate change and eco-

hydrological processes, the GCT was carried out on an annual scale on the precipitation and temperature, NDVI, socioeconomic factors, runoff and sediment variables in the entire Gan River basin. It was found that the influence of the precipitation and temperature on the NDVI was not significant on the annual scale. We can see from Figure 9 that the rural population (RP) had a significant effect on the NDVI changes ($p = 0.08$).

The effect of precipitation on the streamflow was significant ($p < 0.1$). The influence of the NDVI on streamflow on the annual scale was not significant ($p = 0.46$). In addition, the effect of the NDVI on sediment transport ($p = 0.15$) was relatively obvious compared with the effect of the average flow on sediment transport ($p = 0.58$) on the annual scale.

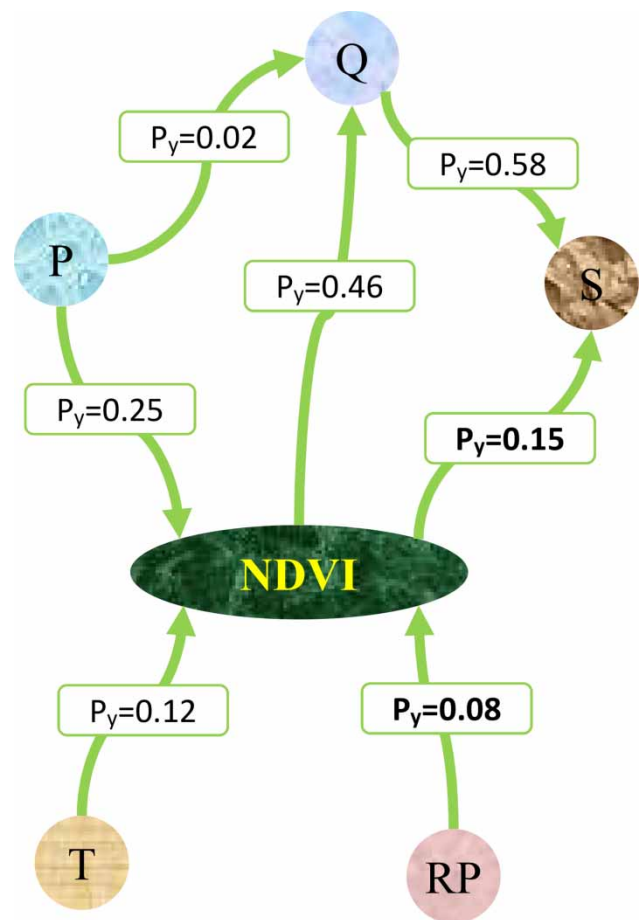


Figure 9 | The p -values of GCT for temperature (T), precipitation (P), NDVI, streamflow (Q), sediment (S), and rural population (RP). The variables indicated by the arrows are the dependent variables. P_y are the p -values on the annual scale, respectively. A smaller p -value indicates a more obvious causal relationship between the variables, and the value of $p < 0.1$ indicates that the causality is significant.

Vegetation restoration does play an important role in alleviating soil erosion and reducing the source of river sediments ($p = 0.15$). The migration of a large number of rural laborers improved vegetation restoration in rural areas, which regulated the amount of sediment to a certain degree.

CONCLUSIONS

In the context of climate change and urbanization, the temperature of the Gan River basin has shown a significant increase. Precipitation has increased in spring and autumn, and decreased in summer and winter. Its vegetation has been continuously restored, and runoff has not changed significantly, but sediment load has shown the downward trend, the rural population showed a decreasing trend. Here, the GCT was used to analyze the statistical causality of these variables. The effect of climate change on the vegetation–hydrological process was found to be not significant on the annual scale, but rather one of the main reasons for the vegetation restoration and sediment load reduction was rural depopulation.

This study can provide reference for studying the rural depopulation effect in other areas of the world, such as India and Vietnam that are rapidly urbanizing. However, a comprehensive analysis of the reasons for the ecological and hydrological changes in the Gan River basin requires further studies in the future.

ACKNOWLEDGEMENTS

This study was supported by the Water Sources Science and Technology Program of Jiangxi (No. KT201614), the Natural Science Foundation of China (No. 51879009), the Second Tibetan Plateau Scientific Expedition and Research Program (STEP, No. 2019QZKK0405), the National Key Research and Development Program of China (No. 2018YFE0196000).

REFERENCES

- Anderson, L. O., Malhi, Y., Aragão, L. E., Ladle, R., Arai, E., Barbier, N. & Phillips, O. 2010 [Remote sensing detection of droughts in Amazonian forest canopies](#). *New Phytologist* **187**, 733–750.
- Attanasio, A., Pasini, A. & Triacca, U. 2012 [A contribution to attribution of recent global warming by out-of-sample Granger causality analysis](#). *Atmospheric Science Letters* **13**, 67–72.
- Attanasio, A., Pasini, A. & Triacca, U. 2013 [Granger causality analyses for climatic attribution](#). *Atmospheric and Climate Sciences* **3**, 515–522.
- Bai, S., Wang, L. & Shi, J. 2012 [Time lag effect of NDVI response to climatic change in Yangtze River Basin](#). *Chinese Journal of Agrometeorology* **33**, 579–586.
- Cai, H., Yang, X., Wang, K. & Xiao, L. 2014 [Is forest restoration in the Southwest China Karst promoted mainly by climate change or human-induced factors?](#) *Remote Sensing* **6**, 9895–9910.
- Cerdà, A. 1997 [Soil erosion after land abandonment in a semiarid environment of southeastern Spain](#). *Arid Land Research and Management* **11** (2), 163–176.
- Cerdà, A., Rodrigo-Comino, J., Novara, A., Brevik, E. C., Vaezi, A. R., Pulido, M., Giménez-Morera, A. & Keesstra, S. D. 2018 [Long-term impact of rainfed agricultural land abandonment on soil erosion in the Western Mediterranean basin](#). *Progress in Physical Geography: Earth and Environment* **42** (2), 202–219.
- Cerdà, A., Ackermann, O., Terol, E. & Rodrigo-Comino, J. 2019 [Impact of farmland abandonment on water resources and soil conservation in citrus plantations in eastern Spain](#). *Water* **11** (4), 824.
- Chen, C. C., Zhang, Y. Q., Xiang, Y., Wang, L. C., Chen, C. C., Zhang, Y. Q., Xiang, Y., Wang, L. C., Chen, C. C. & Zhang, Y. Q. 2014 [Study on runoff responses to land use change in Ganjiang Basin](#). *Journal of Natural Resources* **29**, 1758–1769.
- Cristea, N. C., Lundquist, J. D., Loheide, S. P., Lowry, C. S. & Moore, C. E. 2014 [Modelling how vegetation cover affects climate change impacts on streamflow timing and magnitude in the snowmelt-dominated upper Tuolumne Basin, Sierra Nevada](#). *Hydrological Processes* **28**, 3896–3918.
- Deng, Y. 2010 [Variation of Sediment Discharge of the Drainage Areas of Gan River, Fu River and Liao River From 1957 to 2007 and Its Environmental Significance](#). Nanchang University, China.
- Dickey, D. A. & Fuller, W. A. 1979 [Distribution of the estimators for autoregressive time-series with a unit root](#). *Journal of the American Statistical Association* **74**, 427–431.
- Ding, M. 2017 [The Analysis on the Influence of Urbanization on Urban-Rural Income Gap in Jiangxi Province](#). Jiangxi University of Finance and Economics, China.
- Di Prima, S., Lassabatere, L., Rodrigo-Comino, J., Marrosu, R., Pulido, M., Angulo-Jaramillo, R., Úbeda, X., Keesstra, S., Cerdà, A. & Pirastru, M. 2018 [Comparing transient and steady-state analysis of single-ring infiltrometer data for an abandoned field affected by fire in Eastern Spain](#). *Water* **10** (4), 514.

Anderson, L. O., Malhi, Y., Aragão, L. E., Ladle, R., Arai, E., Barbier, N. & Phillips, O. 2010 [Remote sensing detection of](#)

- Doyle, M., Harbor, J., Rich, C. & AnneSpacie 2000 Examining the effects of urbanization on streams using indicators of geomorphic stability. *Physical Geography* **21**, 155–181.
- Fan, X. & Liu, Y. 2016 A global study of NDVI difference among moderate-resolution satellite sensors. *ISPRS Journal of Photogrammetry and Remote Sensing* **121**, 177–191.
- Fensholt, R. & Proud, S. R. 2012 Evaluation of Earth Observation based global long term vegetation trends – comparing GIMMS and MODIS global NDVI time series. *Remote Sensing of Environment* **119**, 131–147.
- Granger, C. W. J. 1969 Investigating causal relations by econometric models and cross-spectral methods. *Econometrica* **37**, 424–438.
- Hagemann, S., Blome, T., Saeed, F. & Stacke, T. 2014 Perspectives in modelling climate-hydrology interactions. *Surveys in Geophysics* **35**, 739–764.
- Jacobson, C. R. 2011 Identification and quantification of the hydrological impacts of imperviousness in urban catchments: a review. *Journal of Environmental Management* **92**, 1438.
- Kaufmann, R. K., Seto, K. C., Schneider, A., Liu, Z., Zhou, L. & Wang, W. 2007 Climate response to rapid urban growth: evidence of a human-induced precipitation deficit. *Journal of Climate* **20**, 2299–2306.
- Keesstra, S. D., Bouma, J., Wallinga, J., Tittonell, P., Smith, P., Cerdà, A., Montanarella, L., Quinton, J. N., Pachepsky, Y., van der Putten, W. H., Bardgett, R. D., Moolenaar, S., Mol, G., Jansen, B. & Fresco, L. O. 2016 The significance of soils and soil science towards realization of the United Nations Sustainable Development Goals. *Soil* **2**, 111–128.
- Keesstra, S., Mol, G., de Leeuw, J., Okx, J., de Cleen, M. & Visser, S. 2018 Soil-related sustainable development goals: four concepts to make land degradation neutrality and restoration work. *Land* **7** (4), 133.
- Kendall, M. G. 1955 Rank correlation methods. *British Journal of Psychology* **25**, 86–91.
- Kong, D., Miao, C., Borthwick, A. G. L., Lei, X. & Li, H. 2018 Spatiotemporal variations in vegetation cover on the Loess Plateau, China, between 1982 and 2013: possible causes and potential impacts. *Environmental Science and Pollution Research* **25**, 13633–13644. doi:10.1007/s11356-018-1480-x.
- Ledent, & Jacques 1982 Rural-urban migration, urbanization, and economic development. *Economic Development and Cultural Change* **30**, 507–538.
- Leopold, L. 1968 *Hydrology for Urban Planning – A Guidebook on the Hydrologic Effects of Urban Land Use*. U.S. Department of the Interior U.S. Geological Survey Circular. USGS, Washington DC, p. 554.
- Leroux, L., Bégué, A., Seen, D. L., Jolivot, A. & Kayitakire, F. 2017 Driving forces of recent vegetation changes in the Sahel: lessons learned from regional and local level analyses. *Remote Sensing of Environment* **191**, 38–54.
- Liu, X. 2016 *Study on Characteristics of Runoff and Sediment in the Ganjiang River Basin*. Jiangxi Normal University, China.
- Liu, W., Zhan, J., Zhao, F., Yan, H., Zhang, F. & Wei, X. 2019 Impacts of urbanization-induced land-use changes on ecosystem services: a case study of the Pearl River delta metropolitan region, China. *Ecological Indicators* **98**, 228–238.
- Mann, H. B. 1945 Nonparametric tests against trend. *Econometrica* **13**, 245–259.
- Mao, Y., Ye, A. & Xu, J. 2012 Using land use data to estimate the population distribution of China in 2000. *GIScience & Remote Sensing* **49** (6), 822–853.
- Mo, M., Yang, Y., Xiao, S. & Tu, A. 2017 Analysis on characteristics of runoff and sediment and influencing factors in Five Basins of the Poyang Lake. *Research of Soil and Water Conservation* **24**, 197–203.
- Novara, A., Gristina, L., Sala, G., Galati, A., Crescimanno, M., Cerdà, A., Badalamenti, E. & La Mantia, T. 2017 Agricultural land abandonment in Mediterranean environment provides ecosystem services via soil carbon sequestration. *Science of the Total Environment* **576**, 420–429.
- Papagiannopoulou, C., Miralles, D. G., Decubber, S., Demuzere, M., Verhoest, N. E. C., Dorigo, W. A. & Waegeman, W. 2017 A non-linear Granger-causality framework to investigate climate-vegetation dynamics. *Geoscientific Model Development* **10**, 1–24.
- Peng, J. 2015 Analysis of water and sediment variation and influencing factors in Poyang Lake Basin since 1950. *Resources and Environment in the Yangtze Basin* **24**, 1751–1761.
- Price, K. 2011 Effects of watershed topography, soils, land use, and climate on baseflow hydrology in humid regions: a review. *Progress in Physical Geography* **35**, 465–492.
- Pumo, D., Arnone, E., Francipane, A., Caracciolo, D. & Noto, L. V. 2017 Potential implications of climate change and urbanization on watershed hydrology. *Journal of Hydrology* **554**, 80–99.
- Qi, X., Jia, J., Liu, H. & Lin, Z. 2019 Relative importance of climate change and human activities for vegetation changes on China's silk road economic belt over multiple timescales. *Catena* **180**, 224–237.
- Qian, F. 2014 *Study on Factors Influencing Migrant Workers Employment Quality and It's Mechanism –with an Illustration From the Case of Jiangxi Province*. Nanchang University, Nanchang.
- Romero, M. E. N., Martínez, T. L., Regües, D., Monreal, L. R. & Cerdà, A. 2011 Hydrological response and sediment production under different land cover in abandoned farmland fields in a Mediterranean mountain environment. *Boletín De La Asociación De Geógrafos Españoles* **101**, 303–323.
- Romero-Díaz, A., Ruiz-Sinoga, J. D., Robledano-Aymerich, F., Brevik, E. C. & Cerdà, A. 2016 Ecosystem responses to land abandonment in Western Mediterranean Mountains. *Catena* **149**, 824–835.
- Salvadore, E., Bronders, J. & Batelaan, O. 2015 Hydrological modelling of urbanized catchments: a review and future directions. *Journal of Hydrology* **529**, 62–81.
- Sellami, H., Benabdallah, S., La, J. I. & Vanclooster, M. 2015 Quantifying hydrological responses of small Mediterranean

- catchments under climate change projections. *Science of the Total Environment* **543**, 924.
- Shao, J. A., Zhang, S. & Li, X. 2016 Effectiveness of farmland transfer in alleviating farmland abandonment in mountain regions. *Journal of Geographical Sciences* **26**, 203–218.
- Shepard, D. 1968 A two-dimensional interpolation function for irregularly-spaced data. In *Proceedings of ACM National Conference*, pp. 517–524.
- Tang, Z. G., Jin-Hui, M. A., Chao-Kui, L. I., Peng, H. H. & Ji, L. 2016 Spatiotemporal changes of vegetation and the responses to temperature and precipitation in Upper Shiyang River Basin. *Advances in Space Research* **60**, 969–979.
- Wei, X., Liu, W. & Zhou, P. 2013 Quantifying the relative contributions of forest change and climatic variability to hydrology in large watersheds: a critical review of research methods. *Water* **5**, 728–746.
- Wesselink, A., de Vriend, H., Barneveld, H., Krol, M. & Bijker, W. 2009 Hydrology and hydraulics expertise in participatory processes for climate change adaptation in the Dutch Meuse. *Water Science and Technology* **60**, 583–595.
- While, A. & Whitehead, M. 2013 Cities, urbanization and climate change. *Urban Studies* **50**, 1325–1331.
- Wu, D., Zhao, X., Liang, S., Zhou, T., Huang, K., Tang, B. & Zhao, W. 2015 Time-lag effects of global vegetation responses to climate change. *Global Change Biology* **21**, 3520–3531.
- Zhang, H., Jiang, Y., Yang, T., Wang, M., Shi, G. & Ding, M. 2016a Heavy metal concentrations and risk assessment of sediments and surface water of the Gan River, China. *Polish Journal of Environmental Studies* **25**, 1529–1540.
- Zhang, J., Zhang, L. & Xie, S. 2016b Analysis of survey results of soil and water conservation measures in Jiangxi Province. *Subtropical Soil and Water Conservation* **28**, 39–41.
- Zhang, Y., You, Q., Chen, C. & Li, X. 2017 Flash droughts in a typical humid and subtropical basin: a case study in the Gan River Basin, China. *Journal of Hydrology* **551**, 162–176.
- Zhang, S., Li, Z., Hou, X. & Yi, Y. 2019 Impacts on watershed-scale runoff and sediment yield resulting from synergetic changes in climate and vegetation. *CATENA* **179**, 129–138.
- Zheng, H., Fang, S., Yang, J., Xie, S. & Chen, X. 2012 Analysis on evolution characteristics and impacting factors of annual runoff and sediment in the Ganjiang River During 1970–2009. *Journal of Soil and Water Conservation* **26**, 28–32.

First received 29 July 2019; accepted in revised form 15 May 2020. Available online 23 June 2020